Expression pattern of the deoxyribonuclease 1 gene: lessons from the *Dnase1* knockout mouse

Markus NAPIREI[1], Albert RICKEN, Dirk EULITZ, Heiko KNOOP and Hans Georg MANNHERZ

Abteilung für Anatomie und Embryologie, Medizinische Fakultät, Ruhr-Universität Bochum, Universitätsstrasse 150, D-44780 Bochum, Germany

The tissue distribution of deoxyribonuclease 1 (DNASE1, DNase I), a Ca^{2+} and Mg^{2+}/Mn^{2+}-dependent secretory endonuclease, has previously been investigated. However, most of these studies did not account for the existence of different members of the *DNASE1* gene family, did not differentiate between endogenous DNASE1 protein synthesis and its extracellular occurrence or were not performed with methods allowing both a sensitive and a specific detection. Now we re-examined the *DNASE1* gene expression pattern by taking advantage of the *Dnase1* knockout mouse model. Direct comparison of samples derived from wild-type (*Dnase1*$^{+/+}$) and knockout (*Dnase1*$^{-/-}$) mice allowed an unambiguous detection of *Dnase1* gene expression at the mRNA and protein level. For the detection of Dnase1 activity, we developed a highly sensitive nuclease zymogram method. We observed high *Dnase1* gene expression in the parotid and submandibular gland as well as in the kidney and duodenum, intermediate expression in the ileum, mesenterial lymph nodes, liver, ventral prostate, epididymis, ovary and stomach, and low expression in the sublingual, preputial, coagulation and pituitary gland. We report for the first time the lachrymal and thyroid glands, the urinary bladder and the eye to be *Dnase1*-expressing organs as well. Since *Dnase1* knockout mice with the 129xC57Bl/6 mixed genetic background have indicated the protection against an anti-DNA autoimmune response as a new physiological function of Dnase1, knowledge of the physiological sites of its synthesis might prove helpful to find new therapeutic strategies.

Key words: deoxyribonuclease 1 (DNase1), endonuclease, gene expression pattern, systemic lupus erythematosus, tissue distribution.

INTRODUCTION

Deoxyribonuclease 1 (EC 3.1.21.1; DNASE1, DNase I), a Ca^{2+}- as well as Mg^{2+}/Mn^{2+}-dependent endonuclease with an optimum pH around 7.5, hydrolyses double-stranded DNA by introducing single-strand nicks generating 5′-phospho-tri- and/or tetra-oligonucleotides [1,2]. Its molecular mass is approx. 31–34 kDa depending on the amino acid composition and extent of glycosylation, both varying in a tissue- and species-specific manner [3,4]. Dnase1 is a secretory protein containing an N-terminal signal peptide responsible for its translation into the rough endoplasmic reticulum followed by maturation, transportation and secretion through the secretory pathway [5,6]. Since its discovery in the bovine pancreas in 1905 by Sachs [7], DNASE1 has primarily been regarded as a digestive enzyme of the gastrointestinal tract contributing to the supply of oligonucleotides in parallel with their *de novo* synthesis (salvage pathway) [8]. This assumption was supported by the finding of *DNASE1* gene expression in many mammalian organs of the gastrointestinal tract in addition to the pancreas [6,9,10], such as the salivary glands [11], stomach [12] and small intestine [13]. Furthermore, DNASE1 and/or DNASE1-like activities were observed in organs and body fluids different from the gastrointestinal tract. Therefore it was suspected that these nuclease(s) might fulfil additional physiological functions [14–17].

In particular, endogenous DNASE1 has been regarded as a candidate endonuclease facilitating chromatin breakdown during programmed cell death (apoptosis) [18]. Furthermore, we showed that extracellular (serum) DNASE1 participates in the chromatin breakdown of necrotic cells *in vitro*, achieved by its diffusion from the extracellular fluid through the ruptured plasma membrane into the cytoplasm and nucleus of necrotic cells [19]. These results might explain the observation that mice with the mixed 129xC57Bl/6 genetic background lacking *Dnase1* gene (GenBank® accession no. U00478) developed symptoms of the autoimmune disease systemic lupus erythematosus [19]. The predominant symptoms of systemic lupus erythematosus in these animals comprised high titres of ANA (anti-nuclear autoantibodies) directed against nucleosomes and double-stranded DNA and an immunocomplex-mediated glomerulonephritis [20,21]. Therefore Dnase1 harbours a protective function against anti-DNA autoimmunity [22].

During the past few years, members of a *DNASE1* gene family displaying high homology with *DNASE1* were identified in different mammalian species [17]. The two most important variants are (i) the murine *Dnase1l1* gene (*DnaseX*, *Xib*, *DNL1L*) [23–26] and (ii) the murine *Dnase1l3* gene (*Dnase*γ, *LS-DNase*, *nh-DNase*, *DNaseY*) [25,27–30], which share 33.8 and 37.5 % identity to the coding nucleotide sequence of the *Dnase1* gene. At the protein level, Dnase1l1 and Dnase1l3 share 34.5 and 43.3 % identity with the amino acid sequence of Dnase1. Similar to Dnase1, it was assumed that both enzymes might be involved in apoptotic DNA fragmentation; nevertheless, the *in vivo* proof for this assumption is still missing [31,32].

In the present study, we give a detailed analysis of murine *Dnase1* gene expression at the mRNA and protein level. This is not only of interest with respect to Dnase1 and its role in the prevention of anti-DNA autoimmunity, but it also appeared necessary to re-examine critically the previous work on *DNASE1* gene expression in different animal species. Such a re-evaluation seemed necessary because most reports in the past did not account for the existence of other *DNASE1* gene family members and the

Abbreviations used: AP, alkaline phosphatase; ANA, anti-nuclear autoantibodies; Dnase1, deoxyribonuclease 1; DPZ, denaturing SDS/PAGE zymogram; HRP, horseradish peroxidase; NPZ, native PAGE zymogram; PNGase F, peptide N-glycosidase F; rhDNASE1, recombinant human DNASE1; RT, reverse transcriptase; SRED assay, single radial enzyme diffusion assay.

[1] To whom correspondence should be addressed (e-mail markus.napirei@ruhr-uni-bochum.de).

methods used were not always DNASE1-specific. In general, the detection assays have to fulfil two prerequisites: they have to be sensitive and specific. The two main methods used for the detection of DNASE1 or DNASE1-like activities in the past were (i) the SRED (single radial enzyme diffusion) assay [33] and (ii) the DPZ (denaturing SDS/PAGE zymogram) [14]. The SRED assay is a sensitive but not specific method for the detection of nucleolytic activities, whereas the DPZ is specific but insensitive.

In this study, we analysed the tissue distribution of Dnase1 by the highly sensitive NPZ (native PAGE zymogram) and took advantage of the *Dnase1*$^{-/-}$ mouse, allowing a comparison of tissue samples derived from *Dnase1*$^{+/+}$ and *Dnase1*$^{-/-}$ mice. This procedure enables the attribution of a nucleolytic activity unambiguous to Dnase1 and to detect Dnase1 isoforms. The protein studies were verified by a *Dnase1*-specific RT (reverse transcriptase)–PCR analysis. mRNA detection ruled out the possibility of a false positive Dnase1 signal in the NPZ resulting from traces of serum Dnase1. Proceeding as described, we screened 36 murine tissues for *Dnase1* gene expression and classified them into four different expression groups (high, intermediate, low and no detectable expression).

MATERIALS AND METHODS

Materials

Heparin (Liquemin) and rhDNASE1 (recombinant human DNASE1, Pulmozym) were obtained from Hoffmann La Roche (Basel, Switzerland); calf thymus DNA, oligo(dT) primers, BSA, protease inhibitor cocktail and ethidium bromide from Sigma–Aldrich (Deisenhofen, Germany); thioglycollate medium from Becton Dickinson Biosciences (Heidelberg, Germany); Omniscript RT Kit and RNeasy Mini Kit from Qiagen (Hilden, Germany); PCR primers from MWG-Biotech (Ebersberg, Germany); RNAlater from Ambion (Austin, TX, U.S.A.); *Taq* polymerase and prestained protein molecular-mass standards from MBI Fermentas (St. Leon-Rot, Germany); PNGase F (peptide N-glycosidase F) from New England Biolabs (Frankfurt a.M., Germany); polyclonal rabbit anti-bovine pancreas DNASE1 antibody NEO46 from Nordic Immunological Laboratories (Tilburg, Netherlands); goat anti-rabbit Ig AP (alkaline phosphatase)-conjugated antibody, fuchsin substrate–chromogen system and levamisole from DakoCytomation (Hamburg, Germany); goat anti-rabbit IgG HRP (horseradish peroxidase)-conjugated antibody and biotinylated protein ladder detection pack from Cell Signaling Technology (Beverly, MA, U.S.A.); anti-β-actin IgM ascites and goat anti-mouse IgM HRP-conjugated antibody from Oncogene (San Diego, CA, U.S.A.) and the ECL Western-blot analysis system and autoradiography films (Hyperfilm; ECL®) from Amersham Biosciences (Freiburg, Germany).

Animals

Dnase1$^{-/-}$ mice of the inbred strain C57Bl/6 and the outbred strain CD-1 (ICR) were generated by backcrossing 129xC57Bl/6 F2 mice [20] with wild-type mice of the appropriate strain at least ten times. *Dnase1*$^{-/-}$ mice of the inbred strain 129P2/OlaHsd were generated by injecting *Dnase1*$^{-/-}$ 129/E14 embryonic stem cells into blastocytes of the mouse strain 129P2/OlaHsd. Animals were bred in our animal facility, were allowed free access to standard laboratory chow and water and were kept on a light/dark cycle of 12 h. All animal procedures carried out in this work received prior approval by the local animal protection committee and were in agreement with the German law of animal protection.

Sequence data

The following cDNA nucleotide sequences deposited at GenBank® were used: murine *Dnase1* (accession no. D83038), murine *Dnase1l1* (accession no. AX593380) and murine *Dnase1l3* (accession no. AF047355). For protein sequences, we used the SWISS-PROT Protein Sequence database: murine Dnase1 (accession no. P49183), murine Dnase1l1 (protein sequence derived from GenBank® accession no. AX593380) and murine Dnase1l3 (accession no. O55070). For protein and DNA sequence analysis, the DNAstar Lasergene software (DNASTAR, Madison, WI, U.S.A.) was used.

Serum extraction

Mouse blood was collected from ether-anaesthetized animals by cardiac puncture. After coagulation for 12 h at 4 °C, the blood was centrifuged for 10 min at 600 ***g*** and the serum was transferred into a fresh tube.

Preparation of leucocytes and macrophages

Leucocytes

Mice (3-month-old) were anaesthetized with ether; the abdominal cavity and thorax were opened and 100 μl of heparin (Liquemin, 5000 injection units/ml) was injected into the left ventricle. Blood was collected by cardiac puncture, centrifuged for 10 min at 600 ***g*** and the serum supernatant was removed. Leucocytes at the serum–erythrocyte interface (buffy coat) were transferred into a new tube, washed twice with ice-cold PBS (pH 7.0) and sedimented by centrifugation. The remaining erythrocytes were lysed by resuspension and incubation in 1.5 ml of ACK buffer (155 mM NH_4Cl/1 mM $KHCO_3$/0.5 mM EDTA, pH 7.2) for 5 min at room temperature (20 °C). Leucocytes were sedimented and washed twice with PBS. Finally, the cell pellet was lysed in 100 μl of lysis buffer [10 mM Tris/HCl, pH 8.0/20 mM EDTA/0.5 % (v/v) Triton X-100/1 % (v/v) protease inhibitor cocktail].

Macrophages

Mice (3-month-old) received an intraperitoneal injection of 3 ml 3 % (w/v) thioglycollate medium and after 5 days, the mice were killed by cervical dislocation and the abdominal skin was pulled back after making a transverse cut into the inguinal area. Then 10 ml of ice-cold PBS were injected into the abdominal cavity and the peritoneum was massaged to distribute the buffer. After removing the PBS using a syringe, the cells collected were sedimented by centrifugation at 170 ***g*** for 5 min at room temperature. The pellet was resuspended in 5 ml of ACK buffer and incubated for 5 min on a rolling incubator at room temperature to lyse the erythrocytes. Macrophages were sedimented and washed twice with PBS.

Preparation of tissue extracts

Mice (3-month-old) were anaesthetized with ether; the abdominal cavity and thorax were opened by a sagittal cut and 100 μl of heparin was injected into the left ventricle. For complete removal of the blood, the inferior vena cava was opened and the mice were perfused with ice-cold PBS through the left ventricle for 5 min. Subsequently, the organs were removed, frozen in liquid nitrogen and stored at -80 °C. Tissue extracts were prepared by homogenizing the organs in lysis buffer for 30 s using a rotor stator. Cell debris was sedimented by centrifugation at 21 000 ***g***, and the protein content of the supernatants was determined by the standard Bradford procedure [34].

NPZ

For the detection of nucleases, 7.5 % (w/v) polyacrylamide gels containing calf thymus DNA were prepared. The final gel solution (10 ml) consisted of 1.88 ml of a mixture of 38.9 % (w/v) acrylamide and 1.1 % (w/v) *N*,*N*′-methylene-bisacrylamide, 2 ml of 5× electrophoresis buffer (125 mM Tris/1.25 M glycine, pH 8.6), 6 ml water, 50 μl of calf thymus DNA (2 mg/ml) and 50 μl of 10 % (w/v) ammonium persulphate. After addition of 20 μl of *N*,*N*,*N*′,*N*′-tetramethylethylenediamine, gels were polymerized in Mini Protean II electrophoresis chambers (Bio-Rad, Munich, Germany). Protein samples dissolved in loading buffer [50 % (v/v) 1× electrophoresis buffer, 50 % (v/v) glycerol, 0.1 % (w/v) Bromophenol Blue] were loaded on to the gels which were run for 3 h at 90 V. Afterwards, the gels were incubated in reactivation buffer (20 mM Tris/HCl, 5 mM $MgCl_2$, 5 mM $CaCl_2$ and 10 μg/ml ethidium bromide, pH 7.3) at 37 °C for 2–24 h and photographed on a UV-transilluminator.

RT–PCR

Complete RNA was isolated from tissues stored in RNAlater stabilization solution at − 20 °C using the RNeasy Mini Kit (Qiagen) according to the manufacturer's instructions. RNA (2 μg) was employed in a 20 μl of RT reaction using the Omniscript RT Kit from Qiagen and 1.5 μg of oligo(dT) primers (12–18 nt). Subsequently, 2 μl of the RT reaction was set in a PCR. For the detection of *β-actin* cDNA, the N-terminal primer 5′-TTGACATCCGTAAAGACCTCTATGC-3′ (nt 940–964, murine mRNA for *β-actin*, GenBank® accession no. X03672) and the C-terminal primer 5′-ACAGTCCGCCTAGAAGCACTTGCGG-3′ (nt 1217–1993) were used and the PCR programme consisted of an initial 94 °C denaturation step for 1 min, 35 cycles of denaturation for 30 s at 94 °C, annealing for 30 s at 55 °C and elongation for 1 min at 72 °C, as well as a completing elongation step at 72 °C for 5 min. For the detection of the full-length *Dnase1* cDNA (excluding the N-terminal peptide of 22 amino acids), the N-terminal primer 5′-CTGAGAATTGCAGCCTTCAA-3′ (nt 228–247, murine mRNA for *Dnase1*, GenBank® accession no. D83038) and the C-terminal primer 5′-GATTTTTCTGAGTGTCACCTC-3′ (nt 1013–993) were used, and the PCR programme consisted of an initial 94 °C denaturation step for 1 min, 35 cycles of denaturation for 30 s at 94 °C, annealing for 30 s at 55 °C and elongation for 1.5 min at 72 °C as well as a completing elongation step at 72 °C for 10 min. For the detection of the C-terminal part of the *Dnase1* cDNA, the N-terminal primer 5′-CAATATGATGATGGCTGTGAAC-3′ (nt 513–534) and the C-terminal primer 5′-GATTTTTCTGAGTGTCACCTC-3′ (nt 1013–993) were used. The PCR programme was identical to that used for *β-actin*.

Immunoblotting

The extracted protein (40 μg) was suspended in sample buffer, heated for 5 min and subjected to SDS/PAGE (12 % gel) [35], together with a biotinylated protein ladder. Western-blot analysis was performed as described in [36]. Immunodetection of specific antigens was performed using the ECL® chemiluminescence detection system. Anti-DNASE1 antibodies were diluted 1:10 000 and anti-actin IgM ascites 1:5000. A goat anti-rabbit IgG and a goat anti-mouse IgM HRP-linked secondary antibody were employed in a dilution of 1:2000. HRP-linked, anti-biotin antibody was added to the secondary antibodies to detect simultaneously the biotinylated standard proteins. Incubation with antibodies was performed either on a shaker at 4 °C overnight (primary antibodies) or at room temperature for 1 h (secondary antibodies).

Dnase1 immunolocalization in tissue cryo-sections

Tissue samples were removed from killed animals and immersed in a fixative comprising 1 % (w/v) paraformaldehyde and 0.1 % (w/v) picric acid in 0.01 M PBS for 24 h at 4 °C, washed with PBS, immersed in 30 % (w/v) sucrose in PBS overnight at 4 °C and then frozen rapidly in isopentane cooled by liquid nitrogen [13]. Then 8-μm-thick sections were cut, mounted on glass slides, air-dried and stored at − 80 °C. Before use, tissue sections were thawed and immersed in PBS for 5 min and indirect immunohistochemical Dnase1 detection was performed utilizing an AP system. Primary antibodies were diluted 1:100 in PBS, containing 5 % (w/v) BSA. Incubation with the primary antibodies was performed on a shaker in a humid chamber for 1 h at room temperature. Thereafter, the tissue sections were washed three times in PBS for 15 min at room temperature. A goat anti-rabbit antibody conjugated with AP served as a secondary antibody diluted 1:2000 in PBS containing 5 % (w/v) BSA. Incubation conditions and the subsequent washing steps were the same as for the primary antibody reaction. The sites of targeted antigen were visualized with a fuchsin substrate–chromogen system according to the manufacturer's instructions. Levamisole (0.2 mM) was added to block endogenous AP activity. Colour development was followed by light microscopy and stopped when comparative sections of parotid tissue stained with the anti-DNASE1 NEO46 antibody showed a strong reaction. Non-specific staining was assessed by omitting the primary antibody. Finally, the tissue sections were counterstained with haemalaun and covered with coverslips using aqueous-based mounting media.

RESULTS

Detection of Dnase1 activity in murine cells and tissues by the NPZ

In the present study, we compared the nuclease activities of a large number of tissues from wild-type and *Dnase1*$^{-/-}$ mice by the NPZ. The NPZ was carried out at pH 8.6 which guaranteed migration of Dnase1 towards the anode due to (i) its pI of 4.7 and (ii) the fact that its carbohydrate chains may contain acidic sugars such as sialic acid [4]. Furthermore, the existence of a small fraction of phosphorylated mannose residues, typical for the lysosomal trafficking pathway, has been reported [37]. Although the NPZ does not allow the estimation of the molecular mass of the detected nucleases, it is 20–40 times more sensitive than the DPZ (results not shown). In contrast with the SRED assay, the NPZ allows differentiation between nucleases having different migration behaviour. Furthermore, employing this assay to samples from *Dnase1*$^{+/+}$ and *Dnase1*$^{-/-}$ mice enables the attribution of nucleolytic activities definitively to Dnase1 and the detection of Dnase1 isoforms.

We screened 36 tissues of both wild-type and knockout mice for Dnase1 activity. The results shown in Figure 1 are representative for three individual mice analysed. No difference in the expression pattern between the mouse strains C57Bl/6, 129P2/OlaHsd and CD-1 (ICR) were detected (results not shown). Dnase1 activity was identified in several organs of the gastrointestinal tract (parotid, submandibular and sublingual gland, stomach, duodenum, ileum and liver), the urogenital tract (kidney, urinary bladder, epididymis, coagulating gland, ventral prostate, preputial gland and the ovary) and in endocrine tissues like the thyroid and the pituitary gland. Furthermore, Dnase1 activity was detected in the lacrimal gland, the eye and mesenterial lymph nodes. To quantify Dnase1 activity, we applied different amounts of protein of each tissue and determined the minimum amount of protein necessary to obtain a positive nuclease signal after 24 h of incubation. The results are listed in Table 1. The tissues

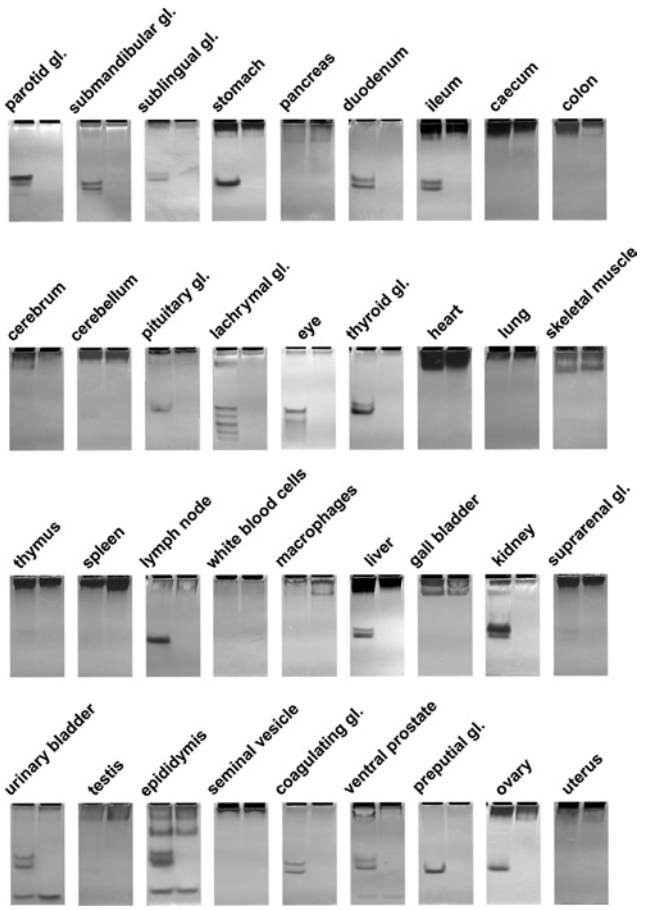

Figure 1 Distribution of Dnase1 activity in murine cells and tissues

Tissue and cell homogenates of *Dnase1*$^{+/+}$ (left gel lanes) and *Dnase1*$^{-/-}$ mice (right gel lanes) were subjected to NPZ. The minimal amount of protein necessary to detect Dnase1 activity by the NPZ after 24 h of incubation was determined and is given in Table 1. A maximum of 80 μg total protein of the homogenates was employed. Most of the organs positively tested for Dnase1 displayed two Dnase1 isoforms. Only one isoform was found in the stomach, pituitary gland, the mesenterial lymph nodes, the preputial gland and the ovary. Besides these two Dnase1 isoforms, additional bands were observed in the lachrymal gland, which most probably represent proteolytic degradation products still harbouring nucleolytic activity (see Figure 2B). Additionally, a faster migrating nuclease in comparison with Dnase1 was detected in the urinary bladder, epididymis and ventral prostate of both *Dnase1*$^{+/+}$ and *Dnase1*$^{-/-}$ mice. Furthermore, a slower migrating activity was observed in the epididymis.

Table 1 *Dnase1* gene expression in murine cells and tissues

Dnase1 activity of different organ extracts was determined using the NPZ. The minimum amount of protein necessary to achieve a nuclease signal after 24 h of incubation is specified as a measure for Dnase1 activity. Detection of Dnase1 enzyme activity was verified by RT–PCR for either the full-length *Dnase1* cDNA or its C-terminal half. Dnase1 activity was not detected by the NPZ in the following organs: pancreas, caecum, colon, rectum, cerebrum, cerebellum, heart, lung, skeletal muscles, thymus, spleen, leucocytes, macrophages, gall-bladder, suprarenal gland, testis, seminal vesicle and uterus (not listed).

	Detection method			
	NPZ		RT–PCR	
Tissue	Detection limit for protein (μg)	Expression factor	Full-length	C-terminus
High expression level				
Parotid gland	0.001	80000	*	*
Lachrymal gland	0.01	8000	*	*
Submandibular gland	0.1	800	*	*
Kidney	0.5	160	*	*
Duodenum	2	40	*	*
Intermediate expression level				
Ileum	20	4	*	*
Lymph node	20	4	*	*
Liver	20	4	*	*
Ventral prostate	20	4	*	*
Epididymis	40	2	*	*
Urinary bladder	40	2	*	*
Ovary	40	2	*	*
Thyroid gland	40	2	*	*
Stomach	40	2	*	*
Low expression level				
Sublingual gland	80	1	†	*
Eye	80	1	†	*
Preputial gland	80	1	†	*
Coagulation gland	80	1	†	*
Pituitary gland	80	1	†	*

* Positive result for *Dnase1* cDNA by RT–PCR.
† Negative result for *Dnase1* cDNA by RT–PCR.

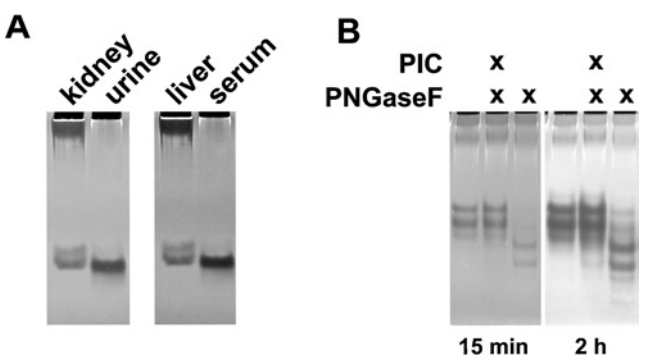

Figure 2 Detection of Dnase1 isoforms

(**A**) Simultaneous investigation of liver and kidney tissue homogenates in comparison with serum and urine of *Dnase1*$^{+/+}$ mice by an NPZ revealed the faster migrating to be the main secretory Dnase1 isoform. (**B**) Extract (5 ng) of the parotid gland of a *Dnase1*$^{+/+}$ mouse was treated with (x) or without 1 unit of PNGase F in the presence (x) or absence of 1 % (v/v) protease inhibitor cocktail (PIC) for 10 min at 37 °C and then analysed by an NPZ. The NPZ gel was developed at 37 °C for 15 min up to 2 h. Note that PNGase F treatment led to the appearance of faster migrating Dnase1 isoforms whose occurrence was inhibited by the addition of PIC. The Dnase1 isoforms therefore seemed to be generated by proteolytic cleavage by proteases contaminating the PNGase F solution and not by deglycosylation.

investigated were divided into four groups according to the *Dnase1* gene expression level (high, intermediate, low and no detectable expression). Besides the detection of Dnase1, additional nuclease activities were detected in some tissue extracts of both *Dnase1*$^{+/+}$ and *Dnase1*$^{-/-}$ mice. A nuclease with faster migration behaviour when compared with Dnase1 was detected in the urinary bladder, epididymis and ventral prostate (Figure 1). Furthermore, a nuclease with a slower migration behaviour was observed in the epididymis (Figure 1).

Detection of Dnase1 isoforms

Most of the wild-type tissues investigated by the NPZ displayed two Dnase1 isoforms, whereas some only displayed the lower migrating form (stomach, pituitary gland, lymph node, preputial gland and ovary; Figure 1). Analysis of extracts from kidney and liver, the most probable sources for urine and serum Dnase1 in comparison with urine and serum, suggested the lower migrating variant to be the secretory isoform (Figure 2A). Two bovine DNASE1 isoforms generated by alternative N-glycosylation were recently detected using the DPZ. It was shown that, in some

bovine organs, Asn-106 was additionally N-glycosylated besides the major site Asn-18 [38]. Since both amino acids are conserved between mouse and cow, we hypothesized that the two isoforms observed were also generated by differential N-glycosylation. The faster migrating isoform might be mono-glycosylated at Asn-18, whereas the slower migrating isoform might be di-glycosylated at Asn-18 and Asn-106. To test this hypothesis, extracts from the *Dnase1*$^{+/+}$ parotid gland were treated with PNGase F. Unfortunately, deglycosylation with PNGase F was not possible employing native protein samples. Instead, we observed an obviously proteolytic cleavage of Dnase1 resulting in a nucleolytic pattern in the NPZ comparable with the pattern obtained for extracts from the lachrymal gland (Figure 1) as verified by performing the deglycosylation reaction in the presence of a protease inhibitor cocktail (Figure 2B).

Distribution of *Dnase1*-specific mRNA in murine cells and tissues

Detection of Dnase1-specific nuclease activity by the NPZ is not sufficient for the conclusion that the enzyme is actually synthesized in cells of the tissue examined, since the presence of serum Dnase1 might cause a false positive signal. Therefore we performed a *Dnase1*-specific RT–PCR. Simultaneous detection of both Dnase1 activity and *Dnase1*-specific mRNA should give a definitive proof of *Dnase1* gene expression in a tissue.

Two strategies of RT–PCR analysis were employed: first, we tried to amplify the complete *Dnase1* cDNA except for the first 22 amino acids (signal peptide) using the primer pair published by Takeshita et al. [15] and second, we tried to amplify the C-terminal half of the *Dnase1* cDNA. Especially for tissues displaying very low Dnase1 activity, the second approach seemed to be necessary to exclude a limited efficiency of the RT reaction. Neither primer pair exhibited nucleotide sequence homology with other members of the *Dnase1* gene family. Furthermore, both primer pairs spanned several intron/exon boundaries, excluding that the amplification products might result from genomic DNA contamination and not from the *Dnase1* cDNA itself. As control for the successful preparation of cDNA, we performed a PCR specific for a part of the *β-actin* gene sequence. Figure 3(A) shows the results for the parotid gland, kidney, duodenum and liver, demonstrating the presence of full-length *Dnase1* cDNA in all samples from wild-type but its complete absence from the knockout tissues. Furthermore, we tested RT samples of heart and spleen derived from *Dnase1*$^{-/-}$ mice for cross-reaction of both *Dnase1* primer pairs with nucleotide sequences of other *Dnase1* gene family members. The heart thereby served as a tissue known for high gene expression of *Dnase1l1* and the spleen for *Dnase1l3* [17]. No amplification product was detected, confirming that both primer pairs are indeed *Dnase1*-specific (results not shown). By employing the full-length *Dnase1* RT–PCR approach, we proved that all tissues displaying high or intermediate Dnase1 specific activity (Table 1) possessed *Dnase1* mRNA (Figure 3B). The amount of *Dnase1* amplification product mirrored the amount of Dnase1 activity estimated in these tissues. The same results were obtained by employing the primer pair for the C-terminal half of the *Dnase1* cDNA (results not shown). In contrast with the tissues of high and intermediate *Dnase1* gene expression, no full-length *Dnase1* cDNA was detected in tissues displaying low Dnase1 activity (results not shown). Nevertheless, the RT samples of all these tissues (Table 1) contained increased amounts of the C-terminal half of the *Dnase1* cDNA (Figure 3C), illustrating that the failure to detect full-length *Dnase1* cDNA might be caused by a very low *Dnase1* mRNA transcription in these organs. Low mRNA levels might be the reason for insufficient generation of full-length *Dnase1* cDNA during the RT reaction. Table 1 gives a comparative summary of all Dnase1 activity and RT–PCR measurements performed.

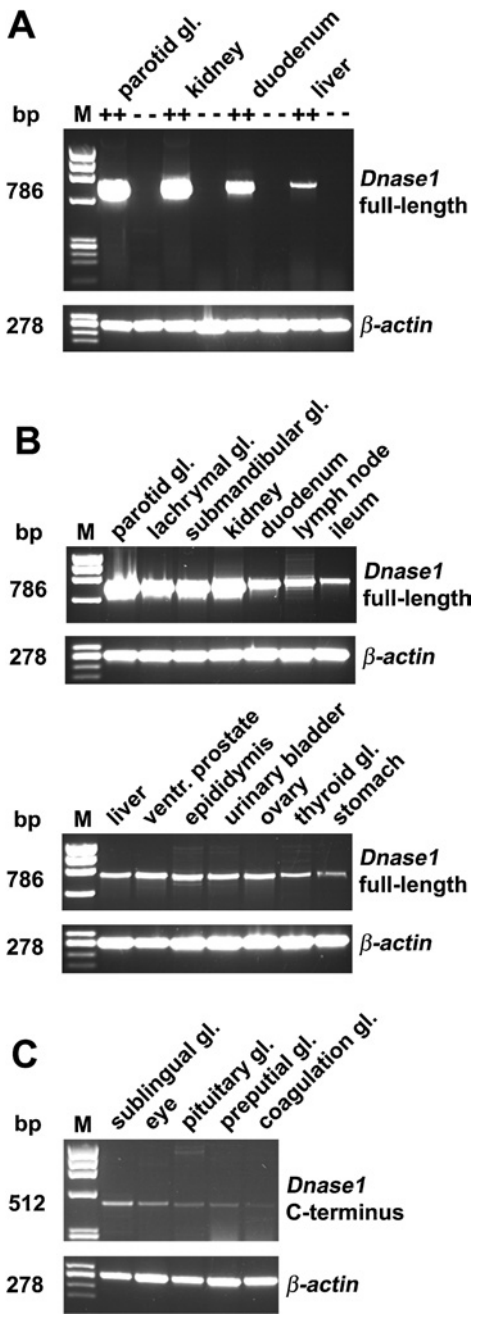

Figure 3 Distribution of *Dnase1*-specific mRNA in murine cells and tissues

(**A**) *Dnase1*-specific RT–PCR of cDNA samples derived from the indicated tissues of *Dnase1*$^{+/+}$ (++) in comparison with *Dnase1*$^{-/-}$ (−−) mice. The PCR encompassed the full-length *Dnase1* cDNA (786 bp), except for the sequence of the first 22 amino acids of the N-terminal signal peptide. The absence of amplification products in samples derived from *Dnase1*$^{-/-}$ mice revealed the *Dnase1* specificity of the primer pair used. The successful preparation of cDNA samples was verified by RT–PCR specific for a part of the *β-actin* cDNA (278 bp). (**B**) cDNA samples of tissues exhibiting high or intermediate Dnase1 activity levels were positively tested for full-length *Dnase1* cDNA by RT–PCR. Although no quantitative PCR was performed, the amount of *Dnase1* cDNA correlated well with the amount of Dnase1 activity measured by NPZ for these tissues (Table 1). (**C**) RT–PCR for the C-terminal half of the *Dnase1* cDNA (512 bp) was performed for tissues displaying Dnase1 activity at the detection limit in the NPZ. M, DNA molecular-mass standard.

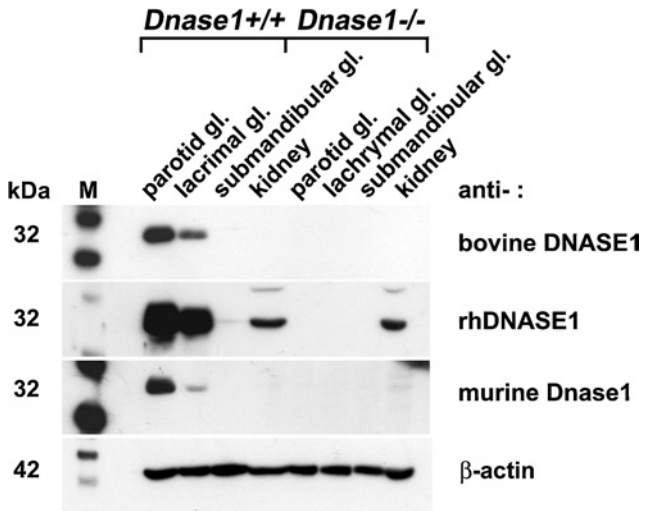

Figure 4 Detection of Dnase1 by immunoblotting

Detection of Dnase1 (32 kDa) in tissue extracts of *Dnase1*$^{+/+}$ in comparison with *Dnase1*$^{-/-}$ mice by immunoblotting was performed using three different antibodies: (i) a polyclonal rabbit anti-bovine pancreas DNASE1 antibody (NEO46), (ii) a rabbit anti-denatured rhDNASE1 antibody and (iii) a monospecific antibody directed against an 11-amino-acid-long peptide of the murine Dnase1 enzyme (residues 66–77). Detection of Dnase1 in tissue extracts of *Dnase1*$^{+/+}$ mice was only possible for the parotid and lacrimal glands, which showed an expression factor of 80 000 and 8000 respectively (Table 1). An expression factor of 800 (submandibular gland) and below (kidney, 160) did not result in a positive immunodetection, except for the submandibular gland and the anti-rhDNASE1 antibody, which displayed the highest sensitivity towards murine Dnase1 of all antibodies tested. A non-specific protein of the same molecular mass as Dnase1 was detected by this antibody in kidney tissue extracts of both *Dnase1*$^{+/+}$ and *Dnase1*$^{-/-}$ mice. As a control for equal protein loading, anti-β-actin-specific immunoblotting was performed in parallel. M, protein molecular-mass standard.

Immunolocalization of murine Dnase1

In a further approach, we tried to immunolocalize Dnase1 in cryo-sections of murine tissues. The antibodies used were NEO46, a commercially available polyclonal rabbit anti-bovine pancreas DNASE1 antibody and a rabbit anti-denatured rhDNASE1 antibody generated by our laboratory. Furthermore, we generated a monospecific antibody directed against an 11-amino-acid-long peptide located at the outer surface of the murine Dnase1 protein (residues 66–77). This peptide has no identity to the amino acid sequence of other members of the Dnase1 family. The generation of the latter antibody will be described in detail elsewhere. The specificity of the antibodies was tested by immunoblotting of tissue extracts. Figure 4 gives a comparative analysis (*Dnase1*$^{+/+}$ versus *Dnase1*$^{-/-}$) of four tissues displaying high *Dnase1* gene expression in wild-type animals (Table 1). All three antibodies employed at the same dilution recognized murine Dnase1 in extracts of the wild-type parotid and lachrymal gland. The intensity of the Dnase1 signal mirrored the Dnase1 activity in these organs using the NPZ (Table 1). The antibody generated against denatured rhDNASE1 displayed the highest sensitivity. Nevertheless, it recognized another protein with approximately an identical molecular mass in kidney extracts of both *Dnase1*$^{+/+}$ and *Dnase1*$^{-/-}$ mice. Using the other antibodies, no anti-Dnase1-reactive band was detected in extracts of wild-type submandibular gland and kidney, although both organs synthesize the enzyme in high amounts. These results demonstrate that the antibodies used are not sensitive enough to detect Dnase1 in organs displaying Dnase1 protein synthesis below that of the lachrymal gland.

The antibodies described were furthermore employed in comparative immunostainings using cryo-sections of organs derived from *Dnase1*$^{+/+}$ and *Dnase1*$^{-/-}$ mice. Figure 5 gives the results obtained for the anti-bovine pancreas DNASE1 antibody NEO46. In accordance with the immunoblots, Dnase1 detection was possible only for the exocrine cells of the wild-type parotid and lachrymal gland. Dnase1-specific staining was not obtained for the submandibular gland (Figure 5) or for other wild-type organs such as the kidney and liver (results not shown). The intensity of Dnase1 detection in the wild-type tissues mirrored the Dnase1 activities measured in these organs.

DISCUSSION

DNASE1 gene expression in tissues of different animal species has been investigated during the last 100 years; however, most reports did not account for the existence of a *DNASE1* gene family. Often, DNASE1-like activities rather than DNASE1 itself were measured, especially when employing the SRED assay. The SRED assay is very sensitive but not DNASE1-specific, i.e. detects the activity of all nucleases displaying the substrate specificity of DNASE1 (double-stranded, protein-free DNA) as well as DNASE1-like biochemical properties (Ca^{2+} and Mg^{2+}/Mn^{2+} dependency, optimum pH approx. 7.5). Therefore the SRED assay was often combined with *DNASE1*-specific RT–PCR analysis. In contrast with the SRED assay, the DPZ is DNASE1-specific because the molecular mass of the nucleases detected can be estimated, but due to the initial denaturation step it is not very sensitive. However, due to the high homology of protein and nucleotide sequence within the *DNASE1* gene family, even the determination of the molecular mass by the DPZ or detection of mRNA by RT–PCR cannot be regarded as a reliable method for the detection of *DNASE1* gene expression. Furthermore, the fact that DNASE1 is the predominant nuclease of most body fluids and secretions may hamper the distinction of endogenous protein synthesis from contamination by exogenous DNASE1.

In the present study, we present an analysis of *Dnase1* gene expression in a large number of murine tissues. The direct comparison between samples derived from *Dnase1*$^{+/+}$ and *Dnase1*$^{-/-}$ mice allowed an unequivocal detection of Dnase1 itself. Detection was performed at both the mRNA and protein level by using *Dnase1*-specific RT–PCR and a newly developed NPZ respectively. Employing these methods, we demonstrate *Dnase1* gene expression in a number of additional organs, such as the thyroid and lachrymal gland, the urinary bladder and the eye. Previously, extensive and detailed studies on murine Dnase1 protein synthesis by employing the SRED assay had been performed by Koizumi [39] and Takeshita et al. [15], whereas Lacks [14] investigated a large number of rat tissues with the DPZ. In contrast with Koizumi [39] and Lacks [14], Takeshita et al. [15] verified their results, in part, by RT–PCR using a primer pair for the detection of full-length *Dnase1* cDNA. A comparative presentation of these reports with the results obtained in the present study is given in Table 2.

Although not all previous studies encompassed the same spectrum of tissues, it is obvious that there is a general agreement, especially for the organs displaying high *Dnase1* gene expression like the parotid and submandibular gland as well as the kidney and small intestine. We describe here the lachrymal gland as a further organ displaying high *Dnase1* gene expression as shown by the NPZ, RT–PCR and immunostaining of the serous exocrine cells. In agreement with Mannherz et al. [40], we immunolocalized Dnase1 in the serous cells of the parotid gland. We calculated an 80 000-fold difference in Dnase1 activity between the parotid gland, the organ with highest activity, and the organs of low activity (see also Table 1). This difference was reflected by the data obtained by immunoblotting and staining. Thus these methods reliably recognized Dnase1 only in the parotid and lachrymal

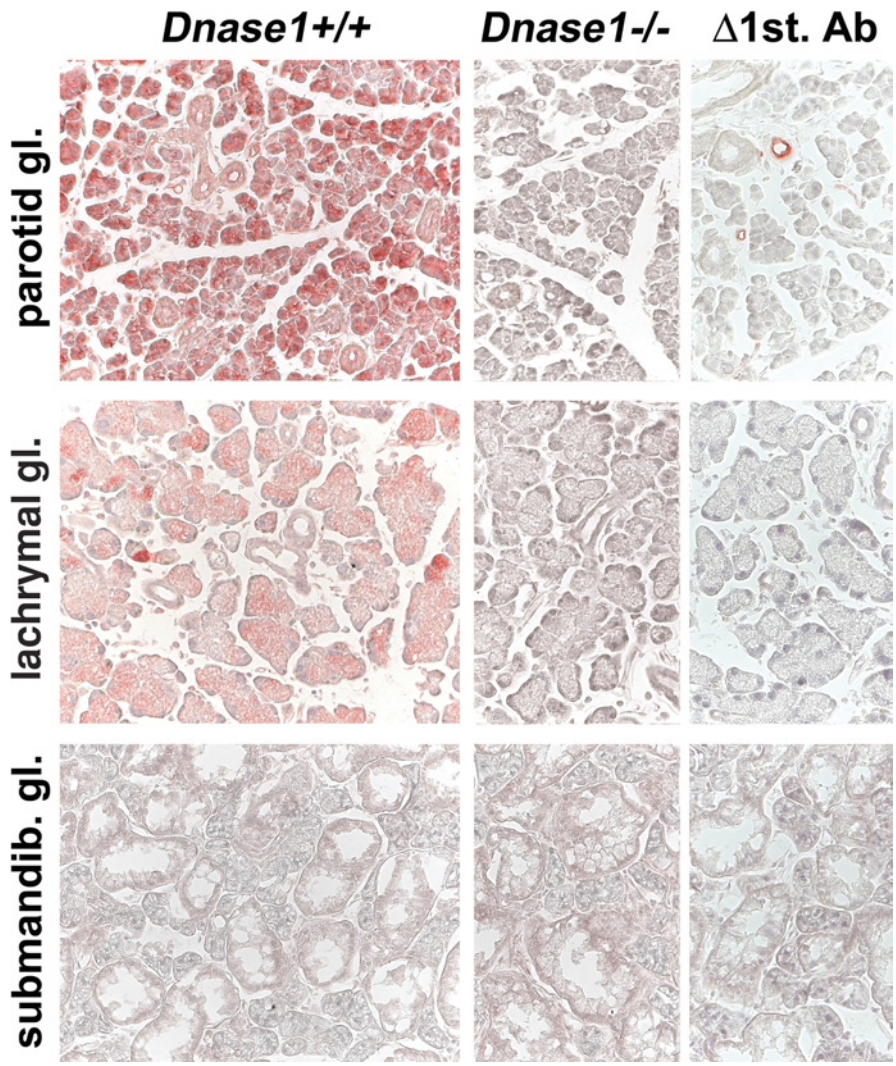

Figure 5 Immunolocalization of Dnase1 in tissue cryo-sections of *Dnase1*$^{+/+}$ mice

In accordance with the immunoblots (Figure 4), Dnase1 detection was possible only for the serous exocrine cells of the parotid and lachrymal gland of *Dnase1*$^{+/+}$ mice. No Dnase1-specific staining was obtained for the submandibular gland. Dnase1 specificity was verified by immunostaining tissue sections derived from *Dnase1*$^{-/-}$ mice. Similarly, omission of the primary antibody (Δ1st.Ab) resulted in loss of the specific immunostaining on tissue sections of *Dnase1*$^{+/+}$ mice. Magnification, × 170.

gland, whereas its low synthesis appeared to preclude its identification in other organs. The presence of DNASE1 in the circulation and the considerable inter-species identity may account for its weak antigenicity and the difficulties to generate highly sensitive antibodies. However, other authors have reported successful immunolocalization of DNASE1 in further organs of other species. This might be explained by the use of different antibodies, species differences in the level of *DNASE1* gene expression, application of different immunostaining techniques or even by false positive detection which might explain some of the contradictory results found in the literature. For the sake of completeness, we will list these results in this discussion. DNASE1 protein synthesis in the small intestine was located to the Paneth cells in human [13], whereas Polzar et al. [41] immunolocalized Dnase1, especially in enterocytes undergoing apoptosis at the tips of villi in the rat. Protein synthesis in the kidney was assumed to occur in the epithelium lining the distal tubules as well as the collecting ducts [42]. So far, no literature exists concerning the subcellular localization of DNASE1 in the submandibular gland.

Intermediate *Dnase1* gene expression was detected in the mesenterial lymph nodes, ventral prostate, epididymis, ovary and stomach. Subcellular localization of Dnase1 in the stomach was previously verified for the chief cells in rat [12], the epithelium of the ventral prostate in the rat [43] and the luteal and granulosa cells of antral follicles as well as the oocytes of the preantral follicles in the rat [44]. Stephan et al. [45] immunodetected Dnase1 in the acrosomic vesicles of rat spermatids and spermatozoa. This observation might explain the *Dnase1* gene expression that we found in the epididymis but is in contrast with the lack of expression in murine testis. In contrast with our study, Takeshita et al. [15] reported *Dnase1* gene expression also for the murine testis and to a lower extent for the epididymis. Still unknown is the cellular source of *Dnase1* gene expression found in the lymph nodes and the liver. In addition to the results published so far, we proved intermediate *Dnase1* gene expression for the urinary bladder and the thyroid gland.

Extremely low *Dnase1* gene expression was detected in the eye, the sublingual, preputial, coagulation and pituitary gland. Cellular sublocalization of this expression so far only exists for the

Table 2 Comparison of studies on *Dnase1* gene expression in the mouse and rat

The results of two previous studies on the *Dnase1* gene expression pattern in the mouse by Koizumi [39] and Takeshita et al. [15] and in the rat by Lacks [14] are compared with the results obtained in the present study (see also Table 1). Lack of Dnase1 activity was verified for the following organs and cell types in the present study: colon, caecum, rectum, gall-bladder, macrophages and leucocytes. –, not determined; neg., no Dnase1 activity detected in the present study.

Tissue	Lacks [14] DPZ (pg/μg of protein)	Takeshita et al. [15] SRED assay ($\times 10^{-4}$ units/g)	Koizumi [39] SRED assay (units/g)	NPZ expression factor
Parotid gland	30000	19000 $\pm$ 3000*	483.78 $\pm$ 102.17	80000*
Lachrymal gland	–	–	–	8000*
Submandibular gland	40	9.8 $\pm$ 8.4*	–	800*
Kidney	8	13 $\pm$ 3.3*	10.54 $\pm$ 1.80	160*
Small intestine	200	3.3 $\pm$ 2.6*	3.15 $\pm$ 1.89	–
Duodenum	–	–	–	40*
Ileum	–	–	–	4*
Lymph node	4	–	–	4*
Liver	$<$ 0.02	1.4 $\pm$ 1.3*	12.19 $\pm$ 1.33	4*
Ventral prostate	1	1.0 $\pm$ 0.53	–	4*
Epididymis	–	0.45 $\pm$ 0.39	–	2*
Stomach	$<$ 0.02	0.10 $\pm$ 0.070*	–	2*
Ovary	–	$<$ 0.05	–	2*
Thyroid gland	–	–	–	2*
Urinary bladder	–	–	–	2*
Sublingual gland	–	37 $\pm$ 18	–	1*
Preputial gland	–	–	30.94 $\pm$ 7.97	1*
Coagulation gland	–	$<$ 0.05	3.92 $\pm$ 3.51	1*
Eye	–	–	–	1*
Pituitary gland	–	–	–	1*
Cerebrum	$<$ 0.02	$<$ 0.05†	0.69 $\pm$ 0.09	neg.
Cerebellum	0.04	$<$ 0.05†	–	neg.
Lung	0.04	$<$ 0.05†	1.91 $\pm$ 0.36	neg.
Heart	1	$<$ 0.05†	1.07 $\pm$ 0.11	neg.
Thymus	$<$ 0.02	$<$ 0.05	2.25 $\pm$ 1.20	neg.
Spleen	$<$ 0.02	$<$ 0.05†	22.88 $\pm$ 6.51	neg.
Pancreas	$<$ 0.02	1.4 $\pm$ 1.2*	1.58 $\pm$ 0.23	neg.
Suprarenal gland	$<$ 0.02	1.3 $\pm$ 0.010	–	neg.
Skeletal muscles	$<$ 0.02	$<$ 0.05	–	neg.
Testis	$<$ 0.02	1.94 $\pm$ 0.53*	–	neg.
Seminal vesicle	0.2	$<$ 0.05	6.08 $\pm$ 1.54	neg.
Uterus	–	2.0 $\pm$ 1.3	–	neg.

* Positive verification of Dnase1 activity measurements by RT–PCR for the *Dnase1* cDNA.
† Negative verification of Dnase1 activity measurements by RT–PCR for the *Dnase1* cDNA.

pituitary gland in human and rat. Shimada et al. [46] immunolocalized DNASE1 in the hormone-secreting cells in the anterior and intermediate lobes.

No detectable *Dnase1* gene expression was demonstrated by our experiments for a variety of tissues, especially of haematopoietic and lymphatic origin. We did not detect Dnase1 in thymus, spleen, leucocytes, macrophages and bone marrow (not shown). It is interesting to note that the *Dnase1* gene family member *Dnase1l3* is highly expressed in most of these tissues [17]. Furthermore, we did not detect Dnase1 in skeletal and cardiac muscles, which are locations of high *Dnase1l1* gene expression [17]. Our NPZ did not allow detection of these Dnase1 family members as they possess a different pI and/or display a different substrate specificity. Lack of *Dnase1* gene expression was additionally shown for the lung, cerebrum and cerebellum, the suprarenal gland, testis, uterus, gall-bladder and parts of the distal gastrointestinal tract like the caecum, colon and rectum. Furthermore, no expression in the pancreas was detected. This is in accordance with the observed differences in the gastrointestinal expression pattern between different mammalian species. Takeshita et al. [47] classified three types: pancreas, parotid and pancreas/parotid (mixed). Rat and mouse are examples exhibiting *Dnase1* gene expression preferentially in the parotid gland. As can be seen from Table 2, there are some discrepancies in our results when compared with previously published results, which may be explained by the inability of the SRED assay to distinguish Dnase1 from Dnase1-like activities.

In summary, our results unambiguously identified *Dnase1* gene expression by employing the *Dnase1* knockout mouse model. We confirmed *Dnase1* gene expression in organs of the gastrointestinal and urogenital tract and, furthermore, demonstrated the lachrymal and thyroid glands, the urinary bladder and the eye as new expression loci. Our results indicated no detectable *Dnase1* gene expression in most of the haematopoietic and lymphatic organs, but verified expression by so far unidentified cells of the lymph nodes. Our results suggest that serum Dnase1 activity could originate from a combined expression in the liver, thyroid gland as well as the pituitary gland. It will be interesting to examine whether *Dnase1* gene expression in these organs and its subsequent transport into the serum can be pharmacologically enhanced, especially in view of its function to provide protection against anti-DNA autoimmunity.

We acknowledge the expert technical assistance of Swantje Wulf and Eva-Maria Konieczny. This work was supported by a grant from the Deutsche Forschungsgemeinschaft (grant no. Ma 807/12-2).

REFERENCES

1 Laskowski, M. (1961) Deoxyribonucleases. In The Enzymes, vol. 5 (Boyer, P. D., Landy, H. and Myrbäck, K., eds.), pp. 123–147, Academic Press, New York
2 Laskowski, M. (1971) Deoxyribonuclease I. In The Enzymes, vol. 4 (Boyer, P. D., Landy, H. and Myrbäck, K., eds.), pp. 289–311, Academic Press, New York
3 Price, P. A., Liu, T. Y., Stein, W. H. and Moore, S. (1969) Properties of chromatographically purified bovine pancreatic deoxyribonuclease. J. Biol. Chem. **244**, 917–923
4 Abe, A. and Liao, T. H. (1983) The immunological and structural comparisons of deoxyribonucleases I. Glycosylation differences between bovine pancreatic and parotid deoxyribonucleases. J. Biol. Chem. **258**, 10283–10288
5 Devillers-Thiery, A., Kindt, T., Scheele, G. and Blobel, G. (1975) Homology in amino-terminal sequence of precursors to pancreatic secretory proteins. Proc. Natl. Acad. Sci. U.S.A. **72**, 5016–5020
6 Kraehenbuhl, J. P., Racine, L. and Jamieson, J. D. (1977) Immunocytochemical localization of secretory proteins in bovine pancreatic exocrine cells. J. Cell Biol. **72**, 406–423
7 Sachs, F. (1905) Über die Nuclease. Hoppe Seylers Z. Physiol. Chem. **46**, 337–353
8 Rudolph, F. B. (1994) The biochemistry and physiology of nucleotides. J. Nutr. **124**, 124S–127S
9 McCarty, M. (1946) Purification and properties of desoxyribonuclease isolated from beef pancreas. J. Gen. Physiol. **29**, 123–139
10 Funakoshi, A., Tsubota, Y., Wakasugi, H., Ibayashi, H. and Takagi, Y. (1977) Purification and properties of human pancreatic deoxyribonuclease I. J. Biochem. (Tokyo) **82**, 1771–1777
11 Kreuder, V., Dieckhoff, J., Sittig, M. and Mannherz, H. G. (1984) Isolation, characterisation and crystallization of deoxyribonuclease I from bovine and rat parotid gland and its interaction with rabbit skeletal muscle actin. Eur. J. Biochem. **139**, 389–400
12 Tsutsumi, S., Kaneko, Y., Asao, T., Kuwano, H., Kudo, S., Takeshita, H., Yasuda, T. and Kishi, K. (2001) DNase I is present in the chief cells of human and rat stomachs. Histochem. J. **33**, 531–535
13 Shimada, O., Ishikawa, H., Tosaka-Shimada, H., Yasuda, T., Kishi, K. and Suzuki, S. (1998) Detection of deoxyribonuclease I along the secretory pathway in Paneth cells of human small intestine. J. Histochem. Cytochem. **46**, 833–840
14 Lacks, S. A. (1981) Deoxyribonuclease I in mammalian tissues. Specificity of inhibition by actin. J. Biol. Chem. **256**, 2644–2648
15 Takeshita, H., Yasuda, T., Nakajima, T., Hosomi, O., Nakashima, Y. and Kishi, K. (1997) Mouse deoxyribonuclease I (DNase I): biochemical and immunological characterization, cDNA structure and tissue distribution. Biochem. Mol. Biol. Int. **42**, 65–75

16 Yasuda, T., Takeshita, H., Nakajima, T., Hosomi, O., Nakashima, Y. and Kishi, K. (1997) Rabbit DNase I: purification from urine, immunological and proteochemical characterization, nucleotide sequence, expression in tissues, relationships with other mammalian DNases I and phylogenetic analysis. Biochem. J. **325**, 465–473
17 Shiokawa, D. and Tanuma, S. (2001) Characterization of human DNase I family endonucleases and activation of DNaseγ during apoptosis. Biochemistry **40**, 143–152
18 Mannherz, H. G., Peitsch, M. C., Zanotti, S., Paddenberg, R. and Polzar, B. (1995) A new function for an old enzyme: the role of DNase I in apoptosis. Curr. Top. Microbiol. Immunol. **198**, 161–174
19 Napirei, M., Wulf, S. and Mannherz, H. G. (2004) Chromatin breakdown during necrosis by serum Dnase1 and the plasminogen system. Arthritis Rheum., in the press
20 Napirei, M., Karsunky, H., Zevnik, B., Stephan, H., Mannherz, H. G. and Moroy, T. (2000) Features of systemic lupus erythematosus in Dnase1-deficient mice. Nat. Genet. **25**, 177–181
21 Jacob, M., Napirei, M., Ricken, A., Dixkens, C. and Mannherz, H. G. (2002) Histopathology of lupus-like nephritis in Dnase1-deficient mice in comparison to NZB/W F1 mice. Lupus **11**, 514–527
22 Lachmann, P. J. (2003) Lupus and desoxyribonuclease. Lupus **12**, 202–206
23 Parrish, J. E., Ciccodicola, A., Wehhert, M., Cox, G. F., Chen, E. and Nelson, D. L. (1995) A muscle-specific DNase I-like gene in human Xq28. Hum. Mol. Genet. **4**, 1557–1564
24 Pergolizzi, R., Appierto, V., Bosetti, A., DeBellis, G. L., Rovida, E. and Biunno, I. (1996) Cloning of a gene encoding a DNase I-like endonuclease in the human Xq28 region. Gene **168**, 267–270
25 Rodriguez, A. M., Rodin, D., Nomura, H., Morton, C. C., Weremowicz, S. and Schneider, M. C. (1997) Identification, localization, and expression of two novel human genes similar to deoxyribonuclease I. Genomics **42**, 507–513
26 Coy, J. F., Velhagen, I., Himmele, R., Delius, H., Poustka, A. and Zentgraf, H. (1996) Isolation, differential splicing and protein expression of a DNase on the human X chromosome. Cell Death Differ. **3**, 199–206
27 Tanuma, S. and Shiokawa, D. (1994) Multiple forms of nuclear deoxyribonuclease in rat thymocytes. Biochem. Biophys. Res. Commun. **203**, 789–797
28 Liu, Q. Y., Pandey, S., Singh, R. K., Lin, W., Ribecco, M., Borowy-Borowski, H., Smith, B., LeBlanc, J., Walker, P. R. and Sikorska, M. (1998) DNaseY: a rat DNaseI-like gene coding for a constitutively expressed chromatin-bound endonuclease. Biochemistry **37**, 10134–10143
29 Zeng, Z., Parmelee, D., Hyaw, H., Coleman, T. A., Su, K., Zhang, J., Gentz, R., Ruben, S., Rosen, C. and Li, Y. (1997) Cloning and characterization of a novel human DNase. Biochem. Biophys. Res. Commun. **231**, 499–504
30 Baron, W. F., Pan, C. Q., Spencer, S. A., Ryan, A. M., Lazarus, R. A. and Baker, K. P. (1998) Cloning and characterization of an actin-resistant DNase I-like endonuclease secreted by macrophages. Gene **215**, 291–301
31 Los, M., Neubuser, D., Coy, J. F., Mozoluk, M., Poustka, A. and Schulze-Osthoff, K. (2000) Functional characterization of DNase X, a novel endonuclease expressed in muscle cells. Biochemistry **39**, 7365–7373
32 Shiokawa, D. and Tanuma, S. (1998) Molecular cloning and expression of a cDNA encoding an apoptotic endonuclease DNaseγ. Biochem. J. **332**, 713–720
33 Nadano, D., Yasuda, T. and Kishi, K. (1993) Measurement of deoxyribonuclease I activity in human tissues and body fluids by a single radial enzyme-diffusion method. Clin. Chem. **39**, 448–452
34 Bradford, M. M. (1976) A rapid and sensitive method for the quantitation of microgram quantities of protein utilizing the principle of protein–dye binding. Anal. Biochem. **72**, 248–254
35 Laemmli, U. K. (1970) Cleavage of structural proteins during the assembly of the head of bacteriophage T4. Nature (London) **227**, 680–685
36 Sambrook, J., Fritsch, E. F. and Maniatis, T. (1989) Molecular Cloning. A Laboratory Manual, Cold Spring Harbor Laboratory Press, Plainview, NY
37 Cacia, J., Quan, C. P., Pai, R. and Frenz, J. (1998) Human DNase I contains mannose 6-phosphate and binds the cation-independent mannose 6-phosphate receptor. Biochemistry **37**, 15154–15161
38 Nishikawa, A. and Mizuno, S. (2001) The efficiency of N-linked glycosylation of bovine DNase I depends on the Asn-Xaa-Ser/Thr sequence and the tissue of origin. Biochem. J. **355**, 245–248
39 Koizumi, T. (1995) Tissue distribution of deoxyribonuclease I (DNase I) activity level in mice and its sexual dimorphism. Exp. Animals **44**, 181–185
40 Mannherz, H. G., Kreuder, V., Koch, J., Dieckhoff, J. and Drenckhahn, D. (1982) The inhibition of bovine and rat parotid deoxyribonuclease I by skeletal muscle actin. A biochemical and immunocytochemical study. Biochem. J. **207**, 305–313
41 Polzar, B., Zanotti, S., Stephan, H., Rauch, F., Peitsch, M. C., Irmler, M., Tschopp, J. and Mannherz, H. G. (1994) Distribution of deoxyribonuclease I in rat tissues and its correlation to cellular turnover and apoptosis (programmed cell death). Eur. J. Cell Biol. **64**, 200–210
42 Zanotti, S., Polzar, B., Stephan, H., Doll, U., Niessing, J. and Mannherz, H. G. (1995) Localization of deoxyribonuclease I gene transcripts and protein in rat tissues and its correlation with apoptotic cell elimination. Histochem. Cell Biol. **103**, 369–377
43 Rauch, F., Polzar, B., Stephan, H., Zanotti, S., Paddenberg, R. and Mannherz, H. G. (1997) Androgen ablation leads to an upregulation and intranuclear accumulation of deoxyribonuclease I in rat prostate epithelial cells paralleling their apoptotic elimination. J. Cell Biol. **137**, 909–923
44 Boone, D. L. and Tsang, B. K. (1997) Identification and localization of deoxyribonuclease I in the rat ovary. Biol. Reprod. **57**, 813–821
45 Stephan, H., Polzar, B., Rauch, F., Zanotti, S., Ulke, C. and Mannherz, H. G. (1996) Distribution of deoxyribonuclease I (DNase I) and p53 in rat testis and their correlation with apoptosis. Histochem. Cell Biol. **106**, 383–393
46 Shimada, O., Suzuki, S., Tosaka-Shimada, H. and Ishikawa, H. (1998) Detection of deoxyribonuclease I in a hormone-secretory pathway of pituitary cells in humans and rats. Cell Struct. Funct. **23**, 49–56
47 Takeshita, H., Mogi, K., Yasuda, T., Nakajima, T., Nakashima, Y., Mori, S., Hoshino, T. and Kishi, K. (2000) Mammalian deoxyribonucleases I are classified into three types: pancreas, parotid, and pancreas-parotid (mixed), based on differences in their tissue concentrations. Biochem. Biophys. Res. Commun. **269**, 481–484

Received 7 January 2004/11 March 2004; accepted 12 March 2004
Published as BJ Immediate Publication 12 March 2004, DOI 10.1042/BJ20040046